Title	An optically tunable wideband optoelectronic oscillator based on a bandpass microwave photonic filter
Author(s)	Jiang, Fan; Wong, Jia Haur; Lam, Huy Quoc; Zhou, Junqiang; Aditya, Sheel; Lim, Peng Huei; Lee, Kenneth Eng Kian; Shum, Perry Ping; Zhang, Xinliang
Citation	Jiang, F., Wong, J. H., Lam, H. Q., Zhou, J., Aditya, S., Lim, P. H., Lee, K. E. K., Shum, P. P.,& Zhang, X. (2013). An optically tunable wideband optoelectronic oscillator based on a bandpass microwave photonic filter. Optics Express, 21(14), 16381-16389.
Date	2013
URL	http://hdl.handle.net/10220/13173
Rights	

An optically tunable wideband optoelectronic oscillator based on a bandpass microwave photonic filter

Fan Jiang,[1,2] Jia Haur Wong,[2] Huy Quoc Lam,[3] Junqiang Zhou,[2] Sheel Aditya,[2] Peng Huei Lim,[2] Kenneth Eng Kian Lee,[3] Perry Ping Shum,[2] and Xinliang Zhang[1,*]

[1]*Wuhan National Laboratory for Optoelectronics, Huazhong University of Science and Technology, Wuhan 430074, China*
[2]*School of Electrical and Electronic Engineering, Nanyang Technological University, 637553 Singapore*
[3]*Temasek Laboratories, Nanyang Technological University, 637553 Singapore*
[*]*xlzhang@mail.hust.edu.cn*

Abstract: An optoelectronic oscillator (OEO) with wideband frequency tunability and stable output based on a bandpass microwave photonic filter (MPF) has been proposed and experimentally demonstrated. Realized by cascading a finite impulse response (FIR) filter and an infinite impulse response (IIR) filter together, the tunable bandpass MPF successfully replaces the narrowband electrical bandpass filter in a conventional single-loop OEO and serves as the oscillating frequency selector. The FIR filter is based on a tunable multi-wavelength laser and dispersion compensation fiber (DCF) while the IIR filter is simply based on an optical loop. Utilizing a long length of DCF as the dispersion medium for the FIR filter also provides a long delay line for the OEO feedback cavity and as a result, optical tuning over a wide frequency range can be achieved without sacrificing the quality of the generated signal. By tuning the wavelength spacing of the multi-wavelength laser, the oscillation frequency can be tuned from 6.88 GHz to 12.79 GHz with an average step-size of 0.128 GHz. The maximum frequency drift of the generated 10 GHz signal is observed to be 1.923 kHz over 1 hour and its phase noise reaches the −112 dBc/Hz limit of our measuring equipment at 10 kHz offset frequency.

OCIS codes: (230.4910) Oscillators; (230.0250) Optoelectronics; (350.4010) Microwaves.

References and links

1. X. S. Yao and L. Maleki, "Optoelectronic microwave oscillator," J. Opt. Soc. Am. B **13**(8), 1725–1735 (1996).
2. X. S. Yao and L. Maleki, "Optoelectronic oscillator for photonic systems," IEEE J. Quantum Electron. **32**(7), 1141–1149 (1996).
3. L. Huo, Y. Dong, C. Y. Lou, and Y. Z. Gao, "Clock extraction using an optoelectronic oscillator from high-speed NRZ signal and NRZ-to-RZ format transformation," IEEE Photon. Technol. Lett. **15**(7), 981–983 (2003).
4. X. S. Yao, L. Maleki, and D. Eliyahu, "Progress in the opto-electronic oscillator - a ten year anniversary review," *in Proceedings of IEEE MTT-S Internatiomal Microwave Symposium Digest* (Fort Worth, TX, 2004), pp. 287–290.
5. X. S. Yao and L. Maleki, "Multiloop optoelectronic oscillator," IEEE J. Quantum Electron. **36**(1), 79–84 (2000).
6. D. Eliyahu, L. Maleki, and Ieee, "Low phase noise and spurious level in multi-loop opto-electronic oscillators," *in Proceedings of IEEE International Frequency Control Symposium & PDA Exhibition Jointly with 17th European Frequency and Time Forum* (Tampa, FL. 2003), pp. 405–410.
7. W. M. Zhou and G. Blasche, "Injection-locked dual opto-electronic oscillator with ultra-low phase noise and ultra-low spurious level," IEEE Trans. Microw. Theory Tech. **53**(3), 929–933 (2005).
8. O. Okusaga, E. J. Adles, E. C. Levy, W. Zhou, G. M. Carter, C. R. Menyuk, and M. Horowitz, "Spurious mode reduction in dual injection-locked optoelectronic oscillators," Opt. Express **19**(7), 5839–5854 (2011).
9. D. Strekalov, D. Aveline, N. Yu, R. Thompson, A. B. Matsko, and L. Maleki, "Stabilizing an optoelectronic microwave oscillator with photonic filters," J. Lightwave Technol. **21**(12), 3052–3061 (2003).

10. A. B. Matsko, L. Maleki, A. A. Savchenkov, and V. S. Ilchenko, "Whispering gallery mode based optoelectronic microwave oscillator," J. Mod. Opt. **50**, 2523–2542 (2003).
11. K. Volyanskiy, P. Salzenstein, H. Tavernier, M. Pogurmirskiy, Y. K. Chembo, and L. Larger, "Compact optoelectronic microwave oscillators using ultra-high Q whispering gallery mode disk-resonators and phase modulation," Opt. Express **18**(21), 22358–22363 (2010).
12. I. Ozdur, D. Mandridis, N. Hoghooghi, and P. J. Delfyett, "Low noise optically tunable opto-electronic oscillator with Fabry-Perot etalon," J. Lightwave Technol. **28**, 3100–3106 (2010).
13. S. L. Pan and J. P. Yao, "Wideband and frequency-tunable microwave generation using an optoelectronic oscillator incorporating a Fabry-Perot laser diode with external optical injection," Opt. Lett. **35**(11), 1911–1913 (2010).
14. W. Z. Li and J. P. Yao, "An optically tunable optoelectronic oscillator," J. Lightwave Technol. **28**(18), 2640–2645 (2010).
15. M. Li, W. Z. Li, and J. P. Yao, "Tunable optoelectronic oscillator incorporating a high-Q spectrum-sliced photonic microwave transversal filter," IEEE Photon. Technol. Lett. **24**(14), 1251–1253 (2012).
16. B. Yang, X. F. Jin, X. M. Zhang, S. L. Zheng, H. Chi, and Y. Wang, "A wideband frequency-tunable optoelectronic oscillator based on a narrowband phase-shifted FBG and wavelength tuning of laser," IEEE Photon. Technol. Lett. **24**(1), 73–75 (2012).
17. J. Q. Zhou, S. N. Fu, F. Luan, J. H. Wong, S. Aditya, P. P. Shum, and K. E. K. Lee, "Tunable multi-tap bandpass microwave photonic filter using a windowed Fabry-Perot filter-based multi-wavelength tunable laser," J. Lightwave Technol. **29**(22), 3381–3386 (2011).
18. J. Capmany, B. Ortega, and D. Pastor, "A tutorial on microwave photonic filters," J. Lightwave Technol. **24**(1), 201–229 (2006).
19. B. Moslehi and J. W. Goodman, "Novel amplified fiber-optic recirculating delay-line processor," J. Lightwave Technol. **10**(8), 1142–1147 (1992).
20. S. Yamashita and Y. Inoue, "Multiwavelength Er-doped fiber ring laser incorporating highly nonlinear fiber," Jpn. J. Appl. Phys. **44**(34), L1080–L1081 (2005).
21. D. Eliyahu, K. Sariri, A. Kamran, and M. Tokhmakhian, "Improving short and long term frequency stability of the opto-electronic oscillator," in *Proceedings of IEEE International Frequency Control Symposium & PDA Exhibition* (New Orleans, LA. 2002), pp. 580–583.
22. K. Volyanskiy, Y. K. Chembo, L. Larger, and E. Rubiola, "Contribution of laser frequency and power fluctuations to the microwave phase noise of optoelectronic oscillators," J. Lightwave Technol. **28**(18), 2730–2735 (2010).

1. Introduction

Featuring extremely low phase noise, high stability and spectral purity, as well as potentially high oscillation frequency, optoelectronic oscillators (OEOs) are of great interest among the research community and have found potential applications in numerous fields such as wireless communication, radar systems, and photonic signal processing [1–4]. In an OEO, a long fiber-optic delay line is usually used as an optical energy storage element for the microwave signal modulated on the optical carrier. A long fiber results in a long energy-decay time and consequently a low phase noise for the microwave signal generated by the OEO [1]. However, utilizing a long fiber inevitably results in narrow frequency spacing between the eigenmodes circulating in the OEO cavity. Thus, generally an ultra-narrow electrical bandpass filter (EBPF) is required for single mode selection. With high frequency narrowband EBPFs being difficult to manufacture and tune, various alternative schemes for OEOs have been proposed with the motivation to overcome this limitation and thus bring out the aforementioned advantageous features of the OEO.

One such improved OEO scheme is the utilization of multi-loop structure which involves combining the high Q factor and larger mode spacing of a long and short feedback loop, respectively [5–8], thus easing the stringent requirements on EBPFs. Structures of multiple optoelectronic loops and dual injection-locked OEO loops have been demonstrated in [5, 6] and [7, 8], respectively and all these schemes feature ultra-low phase noise and spurious level. In practice, however, these schemes are difficult to be implemented as they often require fine loop length and power control for stable operation. Furthermore, the increasing complexity of such OEO structures also restricts wideband frequency tunability of the oscillating signal. An alternative scheme replaces the EBPF with a photonic filter [9], which may either be an optical resonator [10–12] or a microwave photonic filter (MPF) [13–16]. In this scheme, the oscillation frequency of the OEO is either locked to the optical resonator's eigen-frequencies

or is defined by the frequency response of the MPF. While the optical resonator results in a compact OEO and the MPF is able to provide wideband frequency tunability, the phase noise performance of these OEOs is observed to be relatively poor as compared to those in [5–8].

In this paper we propose and experimentally demonstrate a MPF-based single-loop OEO which can generate stable microwave signals with low phase noise and have wideband frequency tunability at the same time. The MPF, which is based on a combination of a finite impulse response (FIR) type MPF and an infinite impulse response (IIR) type MPF, is the key part to realize such an OEO. To avoid confusion, the FIR and IIR MPFs will be mentioned as the FIR and IIR filters, respectively, while their combination is referred to as the MPF. In the proposed OEO, the FIR filter is implemented as a tunable coarse frequency selector which roughly determines the oscillation frequency while the IIR one serves as a fine frequency selector that assists in suppressing the unwanted neighboring frequency components. By replacing the electrical bandpass filter with the cascade MPF, a wide OEO oscillation frequency tuning range from 6.88 GHz to 12.79 GHz has been achieved. The oscillation is stable as well. The maximum frequency drift of the generated 10.03 GHz signal is 1.923 kHz over 1 hour and its phase noise reaches the −112 dBc/Hz limit of our measuring equipment at 10 kHz offset frequency.
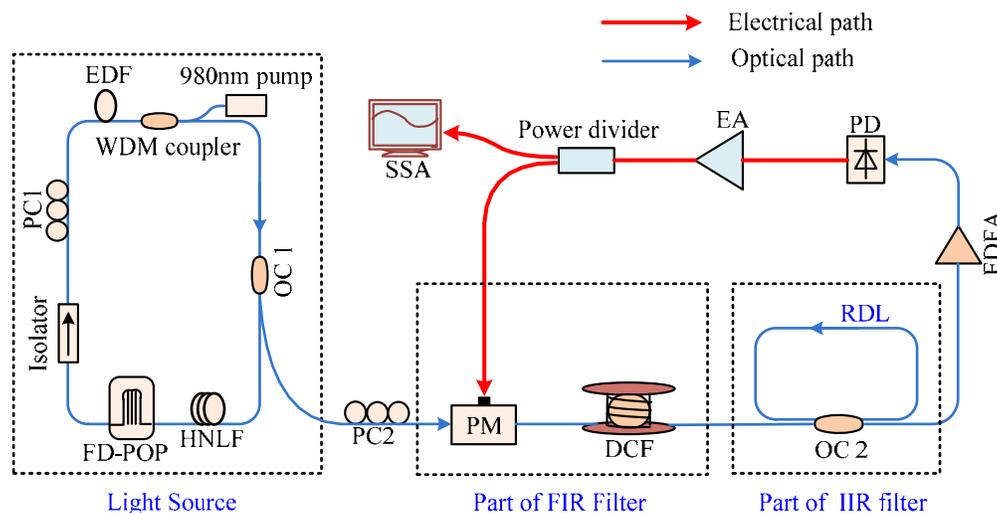
2. Experimental setup and theoretical analysis

Fig. 1. Schematic diagram of the proposed optoelectronic oscillator. PC: polarization controller; EDF: Erbium-doped fiber; WDM: wavelength division multiplexing; FD-POP:Fourier-domain programmable optical processor; HNLF: highly non-linear fiber; OC: optical coupler; PM: phase modulator; DCF: dispersion-compensation fiber; EDFA: Erbium-doped fiber amplifier; PD: Photodetector; EA: electrical amplifier; SSA: signal source analyzer.

Figure 1 depicts the experimental setup of the proposed OEO. The light source, the main part of the FIR filter (without the light source and PD), and the RDL part of the IIR filter are enclosed within the black dash boxes. These three parts together with the PC, EDFA and PD form a cascade microwave photonic filter (MPF). More precisely, the FIR filter is a multi-tap bandpass microwave photonic filter which our research group has previously demonstrated [17] and is realized by a combination of a Fourier-domain programmable optical processor (FD-POP) based multi-wavelength fiber laser, polarization controller (PC2), phase modulator (PM), DCF and PD. On the other hand, the IIR filter is realized by forming a recirculating delay line (RDL) loop after the DCF using a typical 2 × 2 3-dB optical coupler (OC2). Additionally, we have also included an EDFA so as to provide optical gain in the MPF. To

describe the optoelectronic oscillation process in this scheme, we begin at the phase modulator (PM). Here, the input radio frequency (RF) signal first modulates the optical carriers (taps) provided by the multi-wavelength laser. After propagating through the DCF, RDL loop and EDFA, the RF signal is recovered at the PD and filtered accordingly to the response of the MPF. The recovered RF signal is then amplified by an electrical amplifier (EA) and fed back to the RF port of the PM for recirculation, thus forming a complete OEO feedback cavity. The generated RF signal is characterized by a signal source analyzer (SSA) at the 10% output port of the RF power divider. No narrowband EBPF is used in this scheme, and the oscillation frequency corresponds to the passband center of the MPF.

The MPF response in the proposed OEO is a combination of the responses from the FIR and IIR filters [18]. First, the transfer function of the FIR filter can be described as [17]

$$H_1(\omega) \propto \sqrt{\left\{\sum_{n=1}^{N}\left[I_n(\lambda_n)\sin\left(\frac{DL_1\lambda_n^2\omega^2}{4\pi c}\right)\cos(\omega\lambda_n DL_1)\right]\right\}^2 + \left\{\sum_{n=1}^{N}\left[I_n(\lambda_n)\sin\left(\frac{DL_1\lambda_n^2\omega^2}{4\pi c}\right)\sin(\omega\lambda_n DL_1)\right]\right\}^2}, \quad (1)$$

where ω is the electrical angular frequency, n is a positive integer, N is the number of wavelength channels, λ_n is the nth optical wavelength, $I_n(\lambda_n)$ is the tap weight for λ_n, D is the dispersion coefficient, L_1 is the length of the DCF, and c is the speed of light in vacuum. The basic time delay τ_1 of the FIR filter is determined by the time delay difference between adjacent wavelength taps which is induced by chromatic dispersion. So, the free spectral range (FSR) can be expressed as

$$FSR_1 = \frac{1}{\tau_1} = \frac{1}{\Delta\lambda \cdot DL_1}, \quad (2)$$

where $\Delta\lambda$ is the wavelength spacing of the multi-wavelength laser. Since the FD-POP is programmable, the wavelength spacing is a tunable optical parameter in this set-up. Secondly, ignoring any transmission loss, the IIR filter comprising the RDL loop has a transfer function [19]

$$H_2(\omega) = \frac{\kappa + (1-2\kappa)e^{-j\omega\tau_2}}{1 - \kappa e^{-j\omega\tau_2}}, \quad (3)$$

where τ_2 is the loop delay of the RDL loop and κ is the coupling ratio of the optical coupler. Since τ_2 equals the time taken for the optical carriers (taps of the multi-wavelength laser) to travel around the loop once, the FSR of the IIR filter is given as

$$FSR_2 = \frac{1}{\tau_2} = \frac{c}{n_2 L_2}, \quad (4)$$

where n_2 and L_2 are the refractive index and loop length of the RDL loop, respectively. Given the short RDL loop length, the chromatic dispersion of the loop is negligible, and the different taps are treated as experiencing the same time delay. The transfer function of the MPF can thus be expressed directly as the product of their individual transfer functions

$$H(\omega) = H_1(\omega) \cdot H_2(\omega). \quad (5)$$

Next, we take into account the closed loop response of the OEO. After passing through the MPF, the microwave signal is electrically-amplified and fed back to the RF port of the PM, closing the optoelectronic oscillator loop in the process. At any instant of time, the total electric field is the summation of all the fields circulating in the OEO feedback cavity.

Expressing an initial electrical input to be $V_{in}(\omega,t)=A\exp(j\omega t)$, when $H(\omega)G(\omega)$ is lower than unity, the signal measured at the RF input of the PM is then given as

$$V(\omega,t)=V_{in}(\omega,t)\sum_{m=1}^{\infty}\left[H(\omega)G(\omega)\right]^m e^{-j\omega m\tau_3}=\frac{A\exp(j\omega t)}{1-H(\omega)G(\omega)e^{-j\omega\tau_3}},\qquad(6)$$

where A is the amplitude of the input electrical signal, m is an integer, $G(\omega)$ is a simplified gain term related to the EA and RF link loss, and τ_3 is the signal round trip time delay in the OEO feedback cavity. Therefore the RF power can be described as

$$P(\omega)\propto\frac{1}{1+\left[H(\omega)G(\omega)\right]^2-2H(\omega)G(\omega)\cos(\omega\tau_3)}.\qquad(7)$$

The MPF selects one oscillation mode, which corresponds to its passband center, from the eigenmodes spaced by $FSR_3=1/\tau_3$ and suppresses all the other modes.
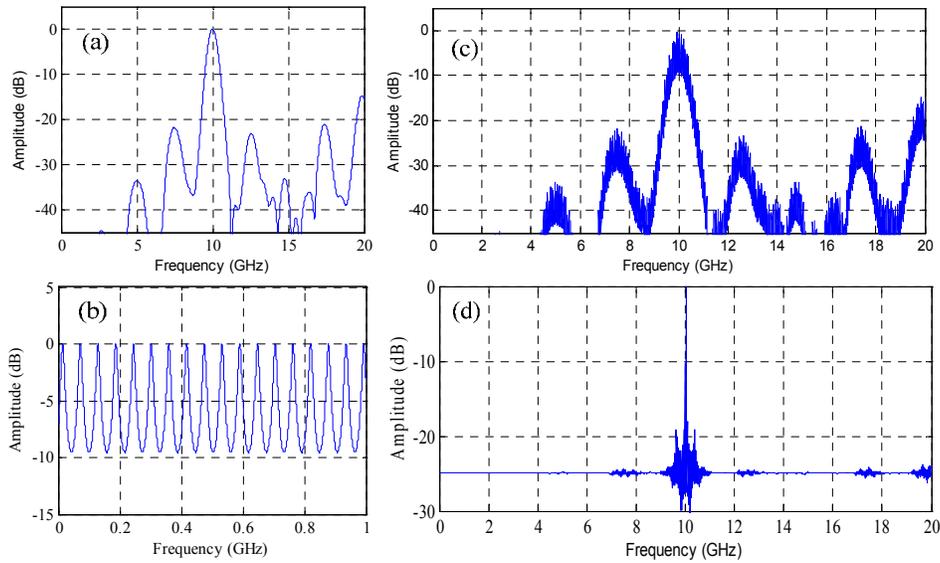

Fig. 2. The simulated filter responses of (a) the FIR filter; (b) the IIR filter; (c) the MPF and (d) the simulated power spectrum of the generated RF signal.

Figure 2 shows the simulation results based on Eqs. (1), (3), (5), and (7) respectively. The individual filter responses of the FIR and the IIR filters are shown in Figs. 2(a) and 2(b) while the response of the MPF is shown in Fig. 2(c). It should be noted that, in our simulation, the tap weight coefficients $I_n(\lambda_n)$ are directly got from the measured output spectrum of the multi-wavelength laser. All the other parameters are set based on the experiment described in the next section. Since both the FSR and the out-of-band rejection ratio of the FIR filter are much larger than that of the IIR filter, the response of the MPF retains the overall shape of the FIR filter, superimposed with small peaks due to the IIR filter. The FIR + IIR combination helps greatly in reducing the effective 3-dB bandwidth of the filter passband, making this MPF a suitable frequency selector in an OEO with a long delay-line. Figure 2(d) illustrates the power spectrum of the generated RF signal corresponding to the filter response in Fig. 2(c). It can be seen that the oscillating frequency f_{osc} roughly corresponds to the passband center of the FIR filter and finely defined by the IIR filter. So the f_{osc} can be estimated and

controlled based on Eq. (2). Precise tuning will need fine delay control to realize exact peak-to-peak match between the FIR filter and the IIR filter.
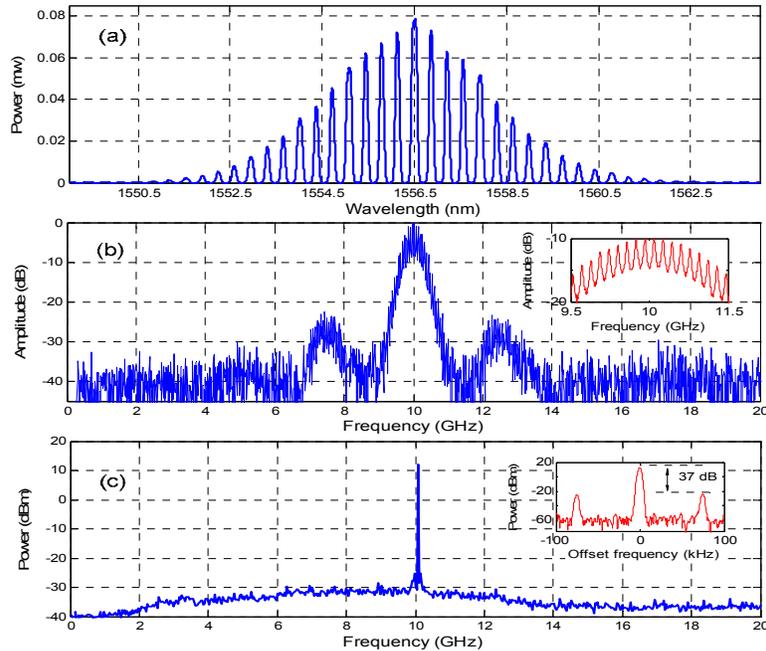
3. Measured results

Fig. 3. Measured results: (a) the laser output spectrum, resolution bandwidth (RBW) = 0.05 nm; (b) the MPF response, inset: a zoomed-in view of the passband center, span = 2 GHz; (c) the spectrum for the generated 10 GHz RF signal, span = 20 GHz, and RBW = 3 MHz, inset: a zoomed-in view of the spectrum, span = 200 kHz, and RBW = 2 kHz.

Experiments have been carried out as a proof-of-concept for the proposed scheme. Critical to this OEO is the output of the FD-POP (Finisar WaveShaper 4000S) based multi-wavelength laser. It is desirable to have as many wavelengths as possible so that the 3-dB bandwidth of the FIR filter can be as narrow as possible. To ensure that the passband of the FIR filter is symmetric in shape and has a high rejection ratio, the power-profile of the multi-wavelength laser has to be set appropriately. Additionally, the wavelength channel spacing of the multi-wavelength laser has to be tuned according to Eq. (2) so that the center frequency of the passband can be swept across the frequencies within the bandwidth of the PD. It is also noted that a higher laser output power enables easier oscillation and better phase noise reduction [1]. Based on the above considerations, we have used a multi-wavelength laser similar to that demonstrated in [17]. A readily-available spool of 2.7 km DCF with a dispersion coefficient −105 ps/km/nm is used as both the dispersion medium for the FIR filter and the delay line for the proposed OEO scheme. Cascading an 8-12 GHz electrical amplifier to a 0-40 GHz electrical amplifier, we are able to provide approximately 20 dB of electrical gain to the RF signals for oscillation. To avoid the DC bias drift issue commonly associated with the use of Mach-Zehnder modulator (MZM), we have implemented a LiNbO$_3$ phase modulator with 40 GHz bandwidth. Before the modulator, a polarization controller (PC2) is used to optimize the polarization of the laser output. To ensure that the first passband of the MPF falls within the 12.5 GHz bandwidth limitation of the PD, we set the wavelength channel spacing to be around 44 GHz so that the passband is centered around 10 GHz. The loop length of the recirculating delay line loop is measured to be 3.6 m.

Figure 3(a) depicts the spectrum of the multi-wavelength laser output and clearly, we observe a windowed power profile and the wavelengths have a uniform spacing of 44 GHz. The number of wavelengths is more than 30 and the laser output power is measured to be about 8.6 dBm. This kind of multi-wavelength fiber laser has potential to lasing over a much broader spectral range [20]. Once the frequency spacing of the FD-POP is set, the peak power fluctuation of each wavelength is measured to be less than 0.4 dB over 15 minutes and no significant spectral fluctuations are observed. The stability of the fiber laser is maintained by the stable response of the FD-POP. The corresponding frequency response of the MPF based on this laser is shown in Fig. 3(b) and is measured using a vector network analyzer. Overall, the passband is observed to have a symmetric shape centered at 10 GHz with more than 25-dB out-of-band rejection ratio. It is worth noting that a highly symmetric shape and a high rejection ratio are critical to selecting the desired mode of oscillation as well as to suppress the unwanted sidemodes on both sides of this centered mode. The two small passbands located beside the center passband are caused by the non-standard window function actually applied to the laser's output power profile by the FD-POP. This in turn is attributed to the wavelength dependent loss of the FD-POP, causing the actual power profile to deviate from the programmed one. The inset of Fig. 3(b), showing a zoomed-in center portion of the MPF passband, reveals that the overall MPF response is in fact, a direct product of the individual responses of the FIR and the IIR filters. The measured filter response matches quite well with the simulation result in Fig. 2(c). The 3-dB bandwidth of the center passband of the FIR filter and that of the IIR filter are measured to be 516 MHz and 13 MHz, respectively. Compared to the scheme in [15] which utilizes a high-Q spectrum-sliced microwave photonic filter in the OEO, our MPF provides a relatively more stable and better shaped filter response due to the utilization of a FD-POP based multi-wavelength laser as the light source as opposed to their use of broadband ASE source. More importantly, with the inclusion of an IIR filter, the overall effective bandwidth of the MPF in our OEO scheme is 13 MHz, much narrower than the 80 MHz in [15]. Using a signal source analyzer (SSA), we measured the generated 10 GHz RF signal and depict its spectrum in Fig. 3(c). Clearly, the oscillation frequency is quite close to the center of the first passband of the FIR filter. Approximately 37-dB sidemode suppression is obtained with the help of the IIR filter. These results verify the correctness of our frequency selection principle and the effectiveness of using such an MPF as the frequency selector in the proposed OEO scheme. Optimizing the length of the EDF in the fiber laser to provide more taps for the FIR-MPF and optimizing the coupling ratio of the IIR-MPF, the cascade MPF can be more selective.

Next, we verify the frequency tunability of our scheme. Based on Eq. (2), by changing the wavelength spacing of the multi-wavelength laser, we are able to tune the passband of the FIR filter to be centered at a desired frequency, which in turn will decide the oscillation frequency. Setting the step size as 1 GHz, we tuned the wavelength channel spacing from 64 GHz to 34 GHz. Correspondingly, the frequency of the generated RF signals can be tuned from 6.88 GHz to 12.79 GHz at an average step size of 0.128 GHz. It should be noted that the step size is limited by the minimum resolution of the FD-POP used. Currently, our demonstrated tuning range is limited by the 8-12 GHz electrical amplifier as it can only provide enough gain for oscillation frequencies within this range. If the electrical amplifier used has a broader gain bandwidth, the tuning range will be wider. The other limitations are the minimum wavelength spacing that can be set by the FD-POP and the maximum total optical bandwidth of the fiber laser output. Figure 4(a) illustrates the spectra for various generated RF signals at about 8, 9, 10 and 11 GHz. The pedestal noise around the signal tone is aroused by the 8-12 GHz EA, and it can be eliminated by improving the gain and bandwidth of the EA. When the FSR of the FIR filter is lower than half of the PD's response bandwidth, the second harmonic of the oscillating frequency is observed. The second harmonic can be eliminated by using a PD with a proper response bandwidth or by adding a suitable electrical filter. Figure 4(b) presents the inverse relationship between the oscillation frequency and the wavelength

spacing. Clearly, there is a good agreement between the measured results (indicated by diamond dots) and the estimated results based on Eq. (2) (shown by red line).
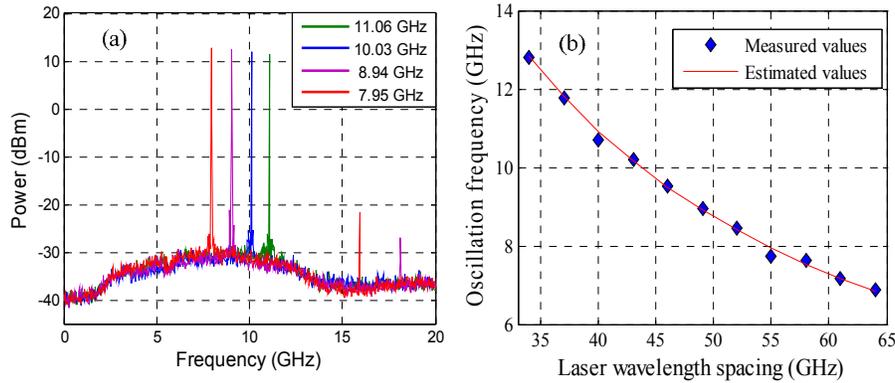

Fig. 4. Frequency tunability of the proposed OEO scheme. (a) Spectra for various generated RF signals, RBW = 1MHz. (b) Correlation of the oscillation frequency and the wavelength spacing.

After verifying the tunability, the stability of the free-running OEO is measured. We have recorded the spectrum for the generated 10 GHz RF signal for over one hour at an interval of ten minutes and the superposition of these spectra is as shown in Fig. 5. The measured maximum oscillation frequency drift over one hour is 1.923 kHz at room temperature and no mode-hopping is observed. In the proposed OEO the oscillation frequency is selected by the microwave photonic filter and the good 0.19 ppm short-term frequency stability for this free running system is a result of the stable response of the filter. The frequency drift is mainly caused by the fiber thermal instability here, so measures can be taken to further improve the system's stability as in [21].
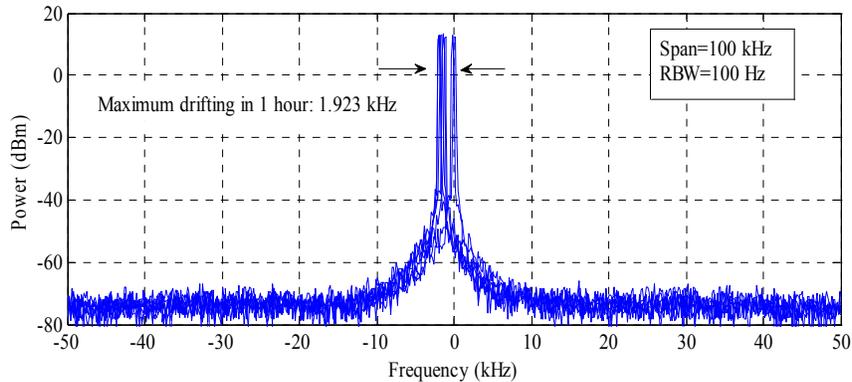

Fig. 5. The superposition of spectra measured in 1 hour.

Lastly, we investigate the phase noise performance of the proposed OEO using the SSA. With the 2.7 km DCF fiber serving as the long delay line, our OEO has a fairly low phase noise performance. The phase noise spectrum of the generated 10.03 GHz signal is measured and depicted in Fig. 6, where a value of −115 dBc/Hz at 10 kHz offset frequency is obtained. It should be noted that the measured phase noise at 10 kHz is currently limited by the SSA (R&S®FSUP26) which has a typical value of −112 dBc/Hz at 10 kHz offset frequency specified in the equipment specifications. Since the measurement results have reached the limit of the equipment, we believe the actual phase noise performance of our OEO is better. It

is also noteworthy that, using dispersion to introduce the filtering effect will impose restriction on the OEO's phase noise performance, since the laser wavelength fluctuations could strongly contribute to the phase noise via the chromatic dispersion of the fiber as analyzed in [22]. This limitation can be compensated by stabilizing the laser. Comparing with traditional OEOs with long fiber delay lines and narrowband electrical bandpass filters [1, 5–8], the OEOs based on MPFs [13–16] usually have the advantages of wideband tunability as well as easier reconfigurability and the disadvantage of degraded phase noise performance. Our proposed scheme makes a good compromise between both features.
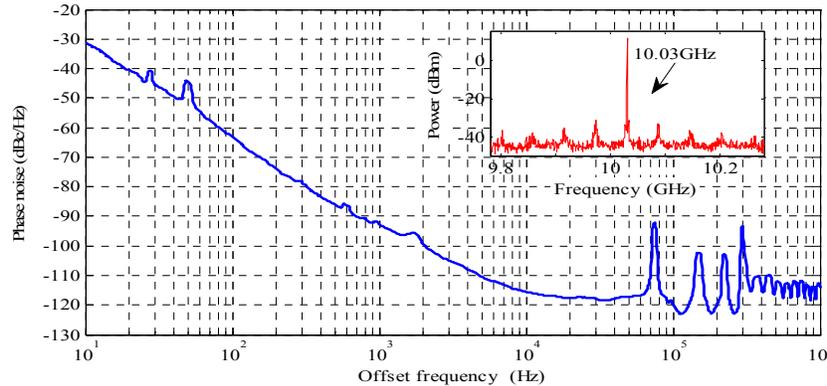

Fig. 6. The measured phase noise for a generated RF signal at 10.03 GHz. Inset: the spectrum of the 10.03 GHz, span = 500 MHz and RBW = 1 MHz.

4. Conclusion

Based on a microwave photonic filter (MPF) implemented by cascading an IIR filter to a tunable FIR filter, we have proposed and experimentally demonstrated a low phase noise OEO with wideband tunability and good stability. Due to the multi-tap bandpass FIR filter with a long dispersion medium, which is fed by a multi-wavelength laser, wideband tuning and low phase noise performance are obtained at the same time for the proposed OEO. The insertion of the IIR filter made by a recirculating delay line loop effectively reduces the 3-dB bandwidth of the MPF, thus ensuring a low spurious level. The oscillation is quite stable with the MPF substituting for the narrowband EBPF in the OEO feedback cavity. The generated RF signal can be easily tuned from 6.88 to 12.79 GHz in steps of 0.128 GHz by changing the laser wavelength spacing. The observed maximum frequency drift for a 10.03 GHz signal is only 1.923 kHz over a period of one hour. The phase noise of the generated 10.03 GHz signal is measured to reaching the sensitivity limit of our measuring equipment with a typical value of −112 dBc/Hz at 10 kHz offset frequency.